Energy Equipment and Systems

Multi objective optimization of the MED-TVC system with exergetic and heat transfer analysis

Authors

Somayyeh Sadri [a]
Ramin Haghighi Khoshkhoo [a*]
Mohammad Ameri [a]

[a] Faculty of Mechanical and Energy Engineering, Shahid Beheshti University, P.O. Box 16765-1719, Tehran, Iran

ABSTRACT

The mathematical model to predict the performance and the exergetic efficiency in a multi-effect desalination system with thermal vapor compression (MED-TVC system) has been presented. The energy and the concentration conservation law were developed for each effect, considering the boiling point elevation and the various thermodynamic losses by developing the mathematical models. These analyses led to the determination of the thermodynamic properties at different points and to the gain output ratio (GOR) values. Then, a heat transfer equation was developed in each effect and the required heat transfer areas were determined. Finally, irreversibility analysis was performed, from which the exergy destruction (considering chemical and physical exergy) and the exergetic efficiency were calculated. To obtain the optimum point of a system, multi-objective optimization was used. Determination of the best trade-off between GOR and heat transfer area was the final goal of this optimization. The optimum design led to a selected system with the lowest heat transfer area (and related cost) and the highest GOR.

1. Introduction

In recent years, the lack of fresh water is a challenge faced by 40% of the world population. Desalination of brackish or saline water is one way to ensure the supply of this vital substance. Ameri et al. [1] provided a thermodynamic model for an MED to produce 2,000 cubic meters per day and analyzed the impact of the number of effects on the desalination performance value. Sayyaadi et al. [2] also developed and optimized a model of an MED-TVC system using thermo-economic

analysis. This developed model was related to the Kish Island's desalination plant. Shakouri et al. [3] developed a model for an MED-TVC system unit so as to connect to Lavan island gas, and then optimized the developed model with thermo-economic analysis. Luo et al. [4] analyzed the gas turbine cycle with a steam-methane reformer to reduce emissions. Zhao et al. [5] used MED for a saline wastewater refinery in China. The thermodynamic model based on mass and energy balances was developed at various stages of desalination. Kamali et al. [6] developed a model to simulate and optimize the thermodynamic MED-TVC system. This model, along with experimental data from the Kish island desalination plant, has

been compared and validated. The model was developed based on the shell-tube exchangers principles, but it dis not include the economic aspects. Shakib et al. [7] evaluated an MED-RO hybrid desalination system and gas turbine cycle for the production of power, heat, and fresh water. Maraver et al. [8] studied a cogeneration system (organic Rankine cycle, MED, and the cooling system) to produce electricity, heat, fresh water, and cooling. Al-Mutaz and Wazeer [9] reviewed the current status of MED-TVC. The primary goal of this paper is to present a preview of some aspects related to the technological theory and parametric study of MED-TVC systems and its development. Kashi [10] investigated the effects of some input parameters on energy efficiency and the produced water in an MED plant. In this study, the mathematical modelling of an MED-TVC system was carried out. Also, the concentration and energy conservation laws were developed for each desalination effect. Based on concentration and energy analyses, the thermodynamic property at each point of a considerable cycle was determined. For the energy and concentration analysis, variable thermodynamic properties were considered. In the next step, the heat transfer analyses of each effect and condenser were performed followed by determination of the required transfer area in each effect and the total required heat transfer area. In the final step, the irreversibility analysis of a mentioned system was performed based on an exergy analysis for each control volume. In the exergetic analysis, the term of chemical exergy was considered and evaluated in an exergy equation. Based on this analysis, the exergy destruction and exergetic efficiency were determined. Finally, to obtain the optimum point of the desalination system, a genetic algorithm, multi-objective, optimization tool was used. Maximization of GOR and minimization of the total heat transfer area were the final goal of optimization. The operational parameters of the desalination system were the decision variables. The results show good improvement in GOR increment and heat transfer area reduction.

Nomenclature

A   heat transfer area (m^2)
B   brine water flow rate(kg/s)
Cp   specific heat (kJ/kg K)
D   distillate water flow rate (kg/s)
e exergy (kW)
F   feed seawater flow rate(kg/s)
h   Enthalpy (kJ/kg)

M   flow rate (kg/s)
P   pressure (kPa)
Q   specific heat consumption (kJ/kg)
S   entropy (kJ/K kg)
T   temperature (K)
U_i overall heat transfer coefficient (kW/m^2 K)
X   salinity (ppm)

Greek letters

Λ latent heat
μ viscosity
μ_0 chemical potential
ρ density

Abbreviations

BPE   boiling point elevation (K)
CR   compression ratio
Ev   entrained vapor
ER   expansion ration
GOR   gain output ratio
LMTD   logarithmic mean temperature difference (K)
NEA   non-equilibrium allowance (K)
ppm   part per million

Subscripts

0   raw water
c   condensing vapor
cw   cooling seawater
f   feed water
p   permeate water
m   motive steam
n   number of effects
s   steam
t   total
v   vapor

2. System description

A schematic view of a parallel-cross (PC) MED-TVC system is shown in Fig. 1. In this paper, the PC configuration of MED-TVC was selected because of its capability in water desalination. The main components of a considerable system were evaporation effects, condenser, flash boxes, and thermal vapour compressor. In this system, the output brine of each effect entered the next effect, and flashed and mixed with the input feed water (F). In PC, the brine flashing started from Effect 2 and carried on until the final effect. The seawater entered the down condenser and absorbed the final effect output steam latent heat. In this procedure, the temperature of seawater reaches the input feed water temperature. A portion of

the warm seawater returned to sea and the rest was used as feed water for the effects. The motive steam entered a desalination system from the external boiler. This steam was condensed in the first effect and returned to the boiler. The input feed water in the first effect was heated by motive steam to top brine temperature (TBT). The feed water evaporated and entered into the next effect as a heat source. The output brine water in Effect 1 entered Effect 2. Finally, the production in the last effect was divided into two parts. One part entered the thermo-compressor and the other entered the down condenser.

3. Energy and exergy balance (mathematical modelling)

The following assumptions have been used to derive the mathematical model: The temperature difference between the effects is equal, the product is salt-free, steady-state operation is being discussed, the feed-flow rate in the effects is the same, the specific heat capacity, boiling point elevation (BPE), and other parameters have been calculated and thermodynamic losses have been studied. The mathematical model was based on concentration, energy, and exergy balances in each effect, thermal vapour compressor, flash box, and condenser.

3.1. Thermal analysis

For the evaluation of mass and energy conservation, and heat transfer calculation, some unknown parameters, such as heat transfer coefficient and physical properties of water, should be determined. These unknown variables have been defined in the following section. The temperature difference between the effects, compressed steam temperature, and last-effect steam temperature can be calculated as follows:

$$\Delta T = \frac{T_1 - T_n}{n-1} \tag{1}$$

$$T_s = T_1 + \Delta T \tag{2}$$

$$T_v = T_n - BPE \tag{3}$$

where, T and n are temperatures in K and the number of effects, respectively. The boiling point elevation (BPE) is related to the dissolved salt value in the water. This factor can be evaluated as given below:

$$
\begin{aligned}
BPE &= X_b \left[B + C X_b \right] \times 10^{-3} \\
B &= \left[6.71 + \left(6.34 \times 10^{-2} \times T_n \right) + \left(9.74 \times 10^{-5} \times T_n^2 \right) \right] \times 10^{-3} \\
C &= [22.238 + \left(9.59 \times 10^{-3} \times T_n \right) + \\
&\quad \left[6.71 + \left(6.34 \times 10^{-2} \times T_n \right) + \left(9.42 \times 10^{-5} \times T_n^2 \right) \right] \times 10^{-8}
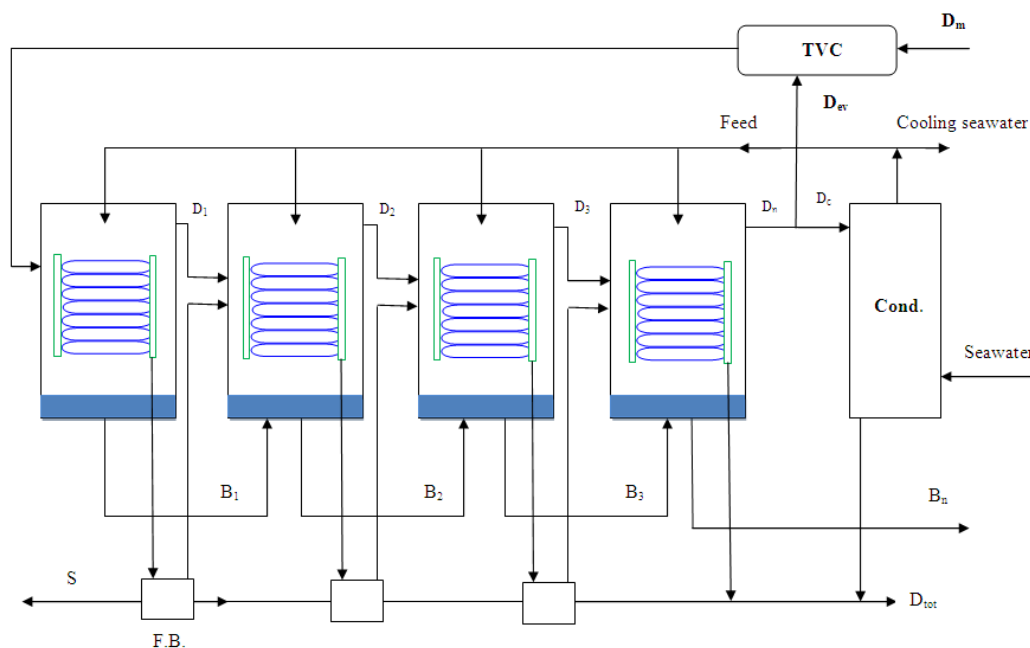\end{aligned} \tag{4}
$$

Fig. 1. Schematic view of a parallel-cross MED-TVC system

The specific heat capacity (c_p) of water can be calculated as follows:

$$c_p = \left[a + b \times T_1 + c \times T_1^2 + d \times T_1^3 \right] \times 10^{-3}$$

$$a = 4206.8 - \left(6.6197 \times S \right) + \left(1.2288 \times 10^{-2} \times S^2 \right)$$

$$b = -1.1262 + \left(5.4178 \times 10^{-2} \times S \right) - \left(2.2719 \times 10^{-4} \times S^2 \right)$$

$$c = \left(1.2026 \times 10^{-2} \right) - \left(5.3566 \times 10^{-4} \times S \right) +$$
$$\left(1.8906 \times 10^{-6} \times S^2 \right) \qquad (5)$$

$$d = \left(6.8777 \times 10^{-7} \right) - \left(1.517 \times 10^{-6} \times S \right) -$$
$$\left(404268 \times 10^{-9} \times S^2 \right)$$

$$S = \frac{X_F}{1000}$$

where, X is the salinity in ppm. Ettouney and El-Dessouky presented a new correlation to evaluate compressed steam pressure P_s and entrained steam pressure P_{ev}, as given below [11]:

$$P_s = 1000 \times \exp\left(\frac{-3892.7}{T_s + 273.15 - 42.6776} + 9.5 \right) \qquad (6)$$

$$P_{ev} = 1000 \times \exp\left(\frac{-3892.7}{T_{vn} + 273.15 - 42.6776} + 9.5 \right) \qquad (7)$$

The expansion ratio (ER) and compression ratio (CR) can be calculated as:

$$ER = \frac{P_m}{P_{ev}} \qquad (8)$$

$$CR = \frac{P_s}{P_{ev}} \qquad (9)$$

The entrainment ratio (Ra) can be calculated as follows [11]:

$$R_a = 0.235 \frac{P_s^{1.19}}{P_{ev}^{1.04}} ER^{0.015} \qquad (10)$$

The amount of entrained vapour was calculated using the following formula.

$$D_{ev} = \frac{D_m}{R_a} \qquad (11)$$

Brine and vapour temperature in each effect can be computed as:

$$T_{i+1} = T_i - \Delta T, \ i = 1,2,\ldots,n \qquad (12)$$

$$T_{vi} = T_i - BPE \qquad (13)$$

The feed seawater flow rate in each effect was calculated by:

$$X_d = 0 \ and \ X_b = 70000, F.X_F = B \times X_b + D * X_d$$
$$,F = B + D, \frac{F}{D} = \frac{X_b}{X_b - X_F} \qquad (14)$$

$$F_i = \frac{F}{n}, i = 1,2,\ldots,n \qquad (15)$$

where, D and B are distilled water and brine water in kg/s, respectively. The condensation temperature of vapor was affected by pressure losses in the demister, and friction in the connecting line and condensation process. This temperature can be calculated as:

$$T_{ci} = T_i - BPE - \Delta T_p - \Delta T_t - \Delta T_c \qquad (16)$$

Steam latent heat can be estimated as follows:

$$\lambda_s = 2501.897149 - 2.407064037 \times T_s + 1.192217 \times 10^{-3} \times T_s^2 - 1.5863 \times 10^{-5} \times T_s^3 \qquad (17)$$

$$\lambda_i = 2501.897149 - 2.407064037 \times T_i + 1.192217 \times 10^{-3} \times T_i^2 - 1.5863 \times 10^{-5} \times T_i^3 \qquad (18)$$

$$\lambda_m = 2501.897149 - 2.407064037 \times T_m + 1.192217 \times 10^{-3} \times T_m^2 - 1.5863 \times 10^{-5} \times T_m^3 \qquad (19)$$

The mass balance in each effect can be calculated by:

$$B_1 = F_1 - D_1 \qquad (20)$$

$$B_i = F_i + B_{i-1} - D_i, \ i = 2,\ldots,n \qquad (21)$$

The salinity of brine at the outlet of each effect can be obtained as given below:

$$X_1 = \frac{F_1}{B_1} \times X_f \qquad (22)$$

$$X_i = \frac{F_i}{B_i} \times X_f + \frac{B_{i-1}}{B_i} \times X_{i-1}, \ i = 2,3,\ldots,n \qquad (23)$$

The energy balance in each effect can be calculated with:

$$D_1 = \frac{1}{\lambda_1} \left[M_s \lambda_s - F_1 \times c_p \left(T_1 - T_f \right) \right] \qquad (24)$$

$$D_i = \frac{1}{\lambda_i} [\left(D_{i-1} + D_{i-1}' \right) \lambda_{i-1} - F_i \times c_p \left(T_i - T_f \right) - B_{i-1} \times c_p \left(T_{i-1} - T_i \right)] \qquad (25)$$

The unknown parameters in the above equations can be evaluated as follows:

$$D'_i = D_{i-1}c_p \frac{T_{v,i-1} - T'_i}{\lambda_i} \tag{26}$$

$$T_{v,i-1} = T_i - BPE \tag{27}$$

$$T'_i = T_{v,i-1} - NEA_i \tag{28}$$

$$NEA_i = 33 \frac{(T_{i-1} - T_i)^{0.55}}{T_{v,i}} \tag{29}$$

where, NEA is the non-equilibrium allowance in k. The vapor generated in the last effect was divided in two parts: condensing vapour D_c and entrained vapour D_{ev}. These can be calculated by:

$$D_c = D_n - D_{ev} \tag{30}$$

The overall heat transfer coefficient U_i was estimated using:

$$U_i = \frac{1939.4 + 1.40562T_i - 0.0207525T_i^2 + 0.0023186T_i^3}{1000} \tag{31}$$

The heat transfer area in each effect (A_i) can be calculated by:

$$A_1 = \frac{(D_s + D_{ev})\lambda_s}{U_1(T_s - T_1)} \tag{32}$$

$$A_i = \frac{D_i\lambda_i}{U_i(T_{c,i} - T_i)}, \ i = 2,3,\ldots,n \tag{33}$$

The total heat transfer area was calculated by the following relation:

$$A_e = A_1 + A_2 + \ldots + A_n = \sum_{i=1}^{n} A_i \tag{34}$$

The logarithmic mean temperature difference (LMTD) and overall heat transfer coefficient of the condenser can be calculated by [11]:

$$(LMTD)_c = \frac{(T_f - T_{cw})}{\ln\left[\dfrac{T_{v,n} - T_{cw}}{T_{c,n} - T_f}\right]} \tag{35}$$

$$U_c = 1.7194 + 3.2063 \times 10^{-2}T_{v,n} - 1.5971 \times 10^{-5}(T_{v,n})^2 + \\ 1.9918 \times 10^{-7}(T_{v,n})^3 \tag{36}$$

The condenser heat transfer area and cooling seawater flow rate was calculated as follows:

$$A_c = \frac{D_c\lambda_n}{U_c(LMTD)_c} \tag{37}$$

$$M_{cw} = \frac{D_c\lambda_n}{c_p(T_f - T_{cw})} \tag{38}$$

The specific heat transfer area is equal to:

$$A_d = \frac{A_e + A_c}{D_t} \tag{39}$$

Finally, the total distilled water and GOR were calculated with the following equations:

$$M_d = \sum_{i=1}^{n} D_i \tag{40}$$

$$GOR = \frac{M_d}{M_m} \tag{41}$$

The specific heat consumption, as an important characteristic of the thermal desalination unit, can be calculated with the following equation:

$$Q = \frac{D_m\lambda_m}{D_t} \tag{42}$$

3.2. Exergy analysis

Exergy is the maximum amount of obtainable work when a system is brought into equilibrium from its initial state to the environmental (dead) state. In the absence of nuclear, magnetic, electrical, and surface tension, the exergy of a system can be divided into four parts:

$$E = E^k + E^{ph} + E^{kpo} + E^{ch} \tag{43}$$

where, $E^k, E^{ph}, E^{kpo}, and \ E^{ch}$ are kinetic exergy, physical exergy, potential exergy, and chemical exergy, respectively. With respect to the selected reference of this study, the kinetic and potential exergy can be neglected from the exergy balance. The exergy balance equation for the control volume can be expanded as follows:

$$\frac{dE}{dt} = \sum\left(1 - \frac{T_0}{T}\right)\dot{Q}_j + \left(\dot{W}_{cv} - P_0\frac{dV_{cv}}{dt}\right) + \\ \sum\dot{m}_i e_i - \sum\dot{m}_e e_e - \dot{E}_D \tag{44}$$

In the absence of output work ($\dot{W}$) and waste heat and considering the steady-state condition, the following equation for exergy balance can be rewritten as:

$$\sum\dot{m}_e e_e - \sum\dot{m}_e e_e = \dot{E}_D \tag{45}$$

where, $\dot{E}_D$ denotes the exergy destruction in this study. Calculating the thermodynamic property of seawater is required for the exergetic analysis

of a considerable system in this study. This thermodynamic property of seawater can be found in the Appendix section [12].

4. Results and discussion

The basic design parameters to analyze the desalination system are shown in Table 1. The distillate water in the system was 10,000 cubic meters per day, in two units. Mathematical calculations were performed based on the design parameters given earlier. The final result of this modelling can be seen in Table 1. The validity of the model was tested using available data from the Tripoli West Plant [13], the results of which are shown in Table 2. To confirm these observations, modelling for another desalination unit was carried out. In addition, the model was validated using data for the Geshm Power and Water Cogeneration Plant (Table 2).

The impact caused by the number of effects on GOR of the Tripoli Plant was evaluated. The results showed that GOR values increased linearly with an increasing number of desalination effects. This occurs because an increase in the number of desalination effects leads to an increase in saline water evaporation and a decrease in the rejection of saline wastewater to the environment. The distribution of GOR values at different TBTs and the number of effects is shown in Fig. 2. The results show that the GOR value increased slowly with an increase in TBT. Moreover, for a specified value for TBT, an increase in the number of effects leads to an increase in the GOR value. With an increase in the number of effects, the possibility of heat exchange between different flows increased, which led to the increase in the amount of fresh water.

Table 1. Input parameters and results of the MED-TVC modeling

Motive steam flow rate, D_m, (kg/s)	8.8
Motive steam pressure, P_m, (kPa)	2300
Feed seawater temperature, T_F, (ºC)	41.5
Cooling water temperature, T_{cw}, (ºC)	31.5
Feed water salinity, X_F, (ppm)	46000
Top brine temperature, T1 (ºC)	60.1
Bottom brine temperature, Tn (ºC)	45.4
Temperature difference, ΔT, $^{\circ}c$	4.9
Entrainment ratio, Ra	1.1265
Expansion ratio, ER	237.2780
Compression ratio, CR	2.6165
Distillate production, Dt, (kg/s)	58.2164
GOR	6.6155
Cooling water flow rate, M_{cw} (kg/s)	409.8
Specific heat consumption, Q, kJ/kg	281.7330
Specific heat transfer area, A_d, m^2/kg/s	253.6623
Exergetic efficiency, %	4.41

Table 2. Mathematical model comparison with two sets of available data — the Tripoli plant, and the Qeshm water and power cogeneration plant

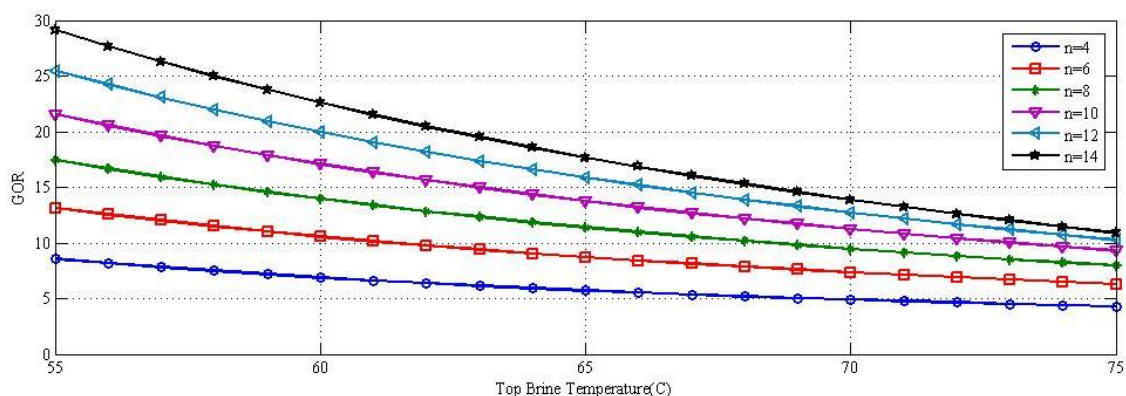| Parameters	Current study	Ref. [14]	Ref. [13]	Current model	Qeshm data[15]
Temperature difference, ΔT, $^{\circ}c$	4.9	4.9	4.9	3.825	$\Delta T_{1-2} = 4$, $\Delta T_{2-3} = 3.7$, $\Delta T_{3-4,4-5} = 3.8$,
Entrainment ratio, Ra	1.1265	1.14	1.14	1.0832	-
Expansion ratio, ER	237.2780	240.9	-	109.1775	-
Compression ratio, CR	2.6165	2.66	-	2.4936	-
Distillate production, Dt, (kg/s)	58.2164	58.02	57.8	50.4131	52.416
GOR	6.6155	6.59	6.51	7.8281	8.26

Fig. 2. Changes in GOR in terms of different top brine temperature

The effect of heating steam temperature on the desalination system's GOR value was investigated. The results show that the GOR value decreased linearly with an increase in the heating steam temperature. This occurs as an increase in the heating steam temperature leads to an increase in the heating steam pressure resulting in an increase in the entrainment ratio value. Thus, for a constant motive flow rate, the entrained vapor flow rate decreased. Due to this the production of fresh water in the first effect reduced. This reduction in the production of fresh water leads to a decrease in the GOR values. The effect of feed water temperature on GOR values can be evaluated. The results show that the increase in feed water temperature caused an increase in the GOR values. Next, the effect of motive steam flow rate on GOR values was analyzed. In constant motive steam, entrained vapour, heating steam pressure, and the expansion ratio remains constant. In this condition, an increase in the motive steam flow rate leads to an increase in the entrained vapour flow rate and distilled water in the first effect. Thus, the total amount of water produced and

the GOR increased. The effect of motive pressure in the thermo-compressor on GOR has been evaluated in Fig. 3. The results show that an increase in the motive steam pressure led to a decrease in the GOR values. This is because the increase in motive steam pressure caused an increase in the expansion ratio in the constant heating steam pressure as well as the entrained vapour pressure. The increase in expansion ratio led to an increase in the entrainment ratio, and hence a decrease in the entrained vapour flow rate. A decrease in the entrained vapour flow rate led to a decrease in the amount of fresh water produced in the first effect, which led to a decrease in the total amount of fresh water and GOR.

It is evident that an increase in TBT leads to a decrease in fresh water production. That is because an increase in TBT leads to an increase in sensible heat. This increase in sensible heat causes an increase in the boiling temperature of the feed water. Thus, the latent heat of steam and total distilled water decreases. The effect of TBT on specific heat consumption can be evaluated.
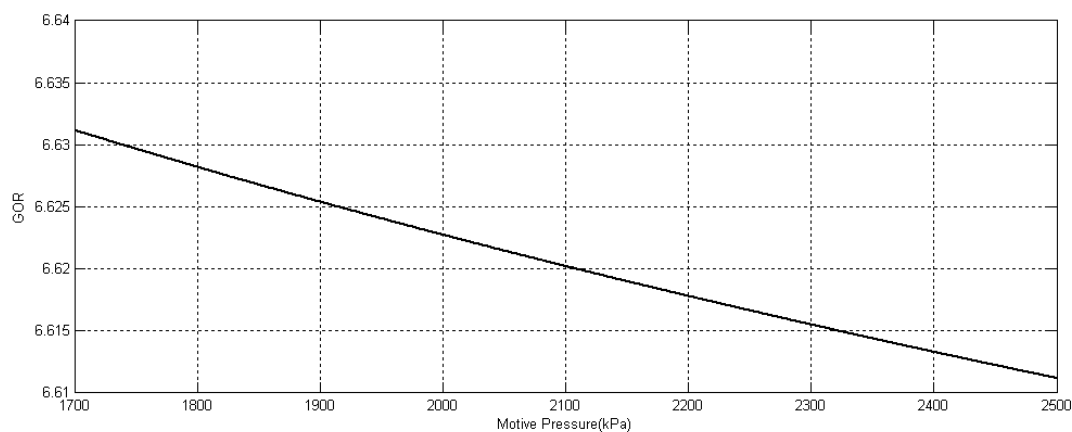

Fig. 3. Changes in GOR in terms of motive steam pressure

The results show that an increase in TBT leads to an increase in specific heat consumption. This occurrs because an increase in TBT causes an increase in vapour pressure and also in the required motive steam. This increase results in an increase in the specific heat consumption. The effect of TBT and the number of effects on specific exergy destruction is shown in Fig. 4. It an also be observed that an increase in the top brine temperature leads to an increase in exergy destruction. At a specified TBT, specific exergy destruction decreased with an increase in the number of effects.

The variation of the specific heat transfer area at the various numbers of effect can be evaluated. The results show that an increase in the number of effects leads to an increase in the rate of the specific heat transfer area. The results of the exergy analysis are shown in Table 3. They show that the exergy destruction in the first effect is higher than in the others. The exergy destruction in different parts of the MED–TVC system is shown in Fig. 5. As evident, effects and leaving streams have the highest and lowest rates of exergy destruction, respectively.
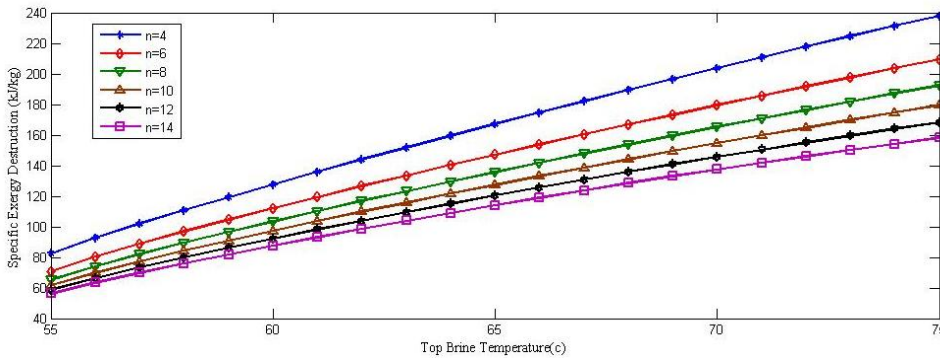

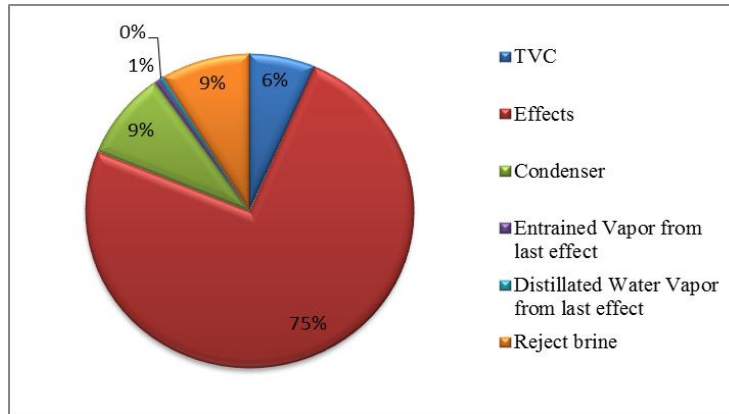**Fig. 4.** The specific exergy changes in terms of top brine temperature

Fig. 5. Exergy destruction on different parts of the MED –TVC system
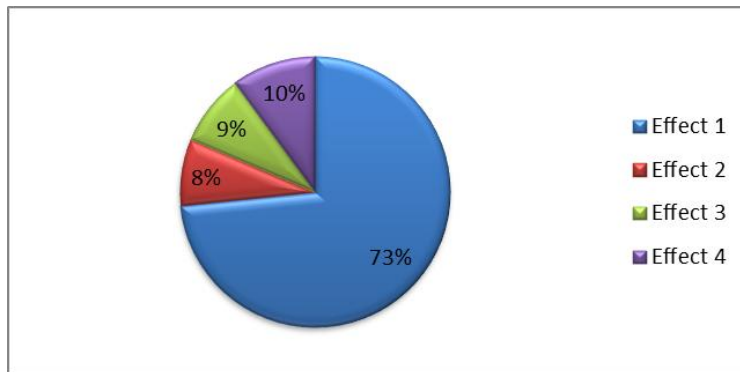

Fig. 6. Exergy destruction on effects

The first effect has the maximum exergy destruction out of all the effects (Fig. 6). Specific exergy destruction and specific exergy consumption, as two key parameters of exergy analysis, can be calculated as show in Table 3.

The variations of exergy destruction per unit of distillate in the condenser, evaporator, and steam ejector, as a function of TBT, are shown in Fig. 7. The results showed that an increase in the TBT in turn increases the exergy destruction per unit of distillate.

To obtain the optimum parameter for considerable systems (Tripoli Plant), two objective functions (GOR and total heat transfer area) were selected.

Multi-objective optimization problems usually exhibit an uncountable set of solutions for assessing the status of vectors, which show the best possible trade-offs in the objective function space. In order to determine a solution that is actually one of the best possible trade-offs, the Pareto optimality is a key concept for expressing the relationship between multi-objective optimization results. GOR is a key goal in the optimization of thermal systems, such as a desalination system. However, increasing the GOR of these thermal systems leads to an increase in heat transfer surfaces and the related capital cost. In this regard, these two functions are used as a goal function in multi-objective optimization. The genetic algorithm optimization toolbox is used due of its capability in multi-objective optimization. The results show that an increase in GOR leads to an increase in the heat transfer area and the related capital cost. The optimum point should be selected from the Pareto front optimization point based on selected decision-making. Hence, the closest point on the Pareto front, with respect to the ideal unreachable point, was selected as an optimum point. To ensure the best selection of the optimum point, the original Pareto front optimum data should be normalized and a normalized Pareto front should be created. Figure 8 shows the normalized Pareto front, which is based on mathematical calculations.

Table 3. Exergy destruction [kW] and specific exergy parameters in the Tripoli plant [kJ/kg]

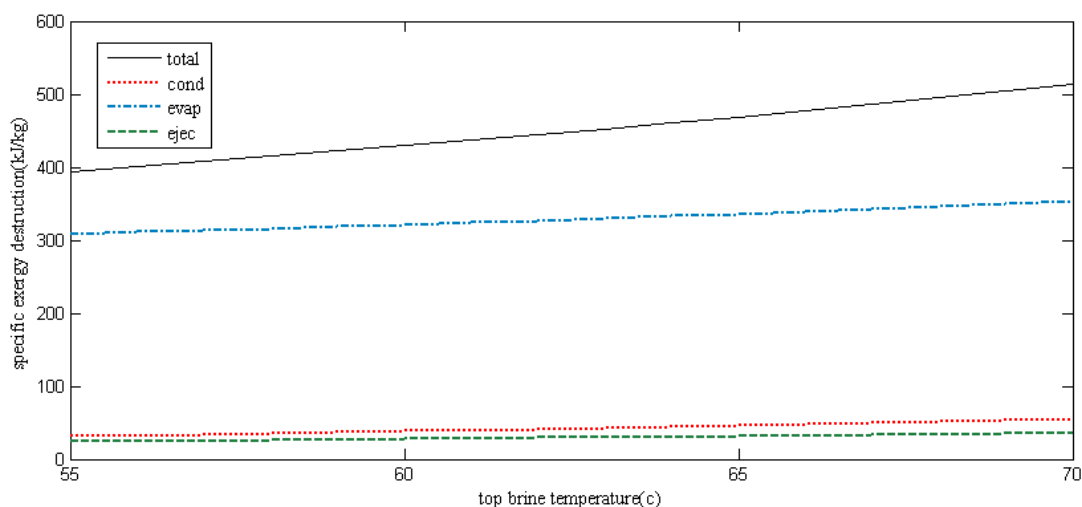| Total	Leaving streams		ev	Condenser	All effects	Effects				TVC	specific exergy destruction	specific exergy consumption
	B_n	D_c				4	3	2	1			
25034	2200.2	121.6	140.2	2247.3	18712	1882	1606	1491	13732	1613	430	361.8

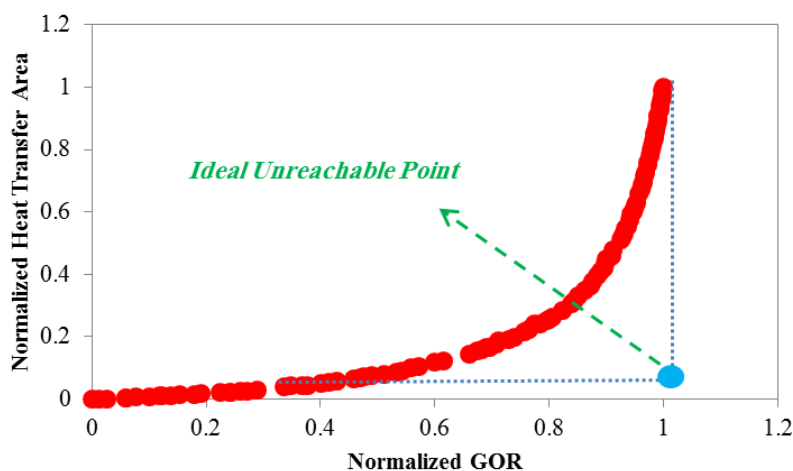**Fig. 7.** Variations in exergy destruction per unit distillate in condenser, evaporator, and steam ejector

Fig. 8. The normalized Pareto front in considerable multi-objective optimization

The optimum goal functions and decision variables are listed in Table 4. These results show that with multi-objective optimization, GOR increased by about 11.32 % (actual percent) with respect to the base design. In addition, the total heat transfer area decreased by about 17.29 % (relative percent) with respect to the base design. Exergetic efficiency was reached at 4.71%.

Table 4. Optimum point data

Parameter	Optimum values
GOR	7.3648
Heat transfer area (m^2)	12235.98
BBT($^\circ c$)	47.79
TBT($^\circ c$)	55.64
Feed water temperature ($^\circ c$)	39.93
Steam motive pressure (kPa)	1917.6
Steam motive flow rate (kg/s)	3.2738

5. Conclusion

In this paper, the MED-TVC system was analyzed for its energy, heat transfer, and exergy approach. Based on the derived mathematical model, the effects of design parameters on GOR, distilled water production, energy consumption, and exergy destruction were evaluated. The results showed that exergy destruction in the first effect was higher than in other effects. Among the effects of exergy destruction, 73% are related to the first effect. Based on multi-objective optimization, the optimum point of the highest GOR and lowest

heat transfer area (and related cost) was determined. The optimal result shows an 11.32% increment in GOR. Analysis of the MED-TVC system in the Tripoli Plant showed that evaporators are the main sources of exergy destruction. Therefore, efforts should be directed towards minimizing these losses by improving the design of these components.

References

[1] Ameri M., Seif Mohammadi S., Hosseini M., Seifi M., Effect of Design Parameters on Multi Effect Desalination System Specifications, Desalination (2009) 245: 266-283.
[2] Sayyaadi H., Saffari A., Mahmoodian A. Various Approaches in Optimization of Multi Effect Distillation Systems Using a Hybrid Meta-Heuristic Optimization Tool, Desalination (2010) 254: 138-148.
[3] Shakouri M., Ghadamian H., Sheiholeslami R., Optimal Model for Multi Effect Desalination System Integrated with Gas Turbine, Desalination (2010) 260: 254-263.
[4] Luo C., Zhang N., Loir N., Lin H., Proposal and Analysis of a Dual Purpose System Integrating a Chemically Recuperated Gas

Turbine Cycle with Thermal Seawater Desalination, Energy (2011) 36: 3791-3803.

[5] Zhao D., Xue J., Li S., Sun H., Zhang Q., Theoretical Analysis of Thermal and Economical Aspects of Multi Effect Distillation Desalination dealing with High Salinity Wastewater, Desalination (2011) 273: 292-298.

[6] Kouhikamali R., Sanaei M., Mehdizadeh M., Process Investigation of Different Locations of Thermo Compressor suction in MED-TVC Plants, Desalination (2011) 280: 134-138.

[7] Shakib S. E., Amidpour M., Aghanajafi C., Simulation and Optimization of Multi Effect Desalination Coupled to a Gas turbine Plant with HRSG Consideration, Desalination (2012) 285: 366-376.

[8] Maraver D., Uche J., Royo J., Assessment of High Temperature Organic Rankine Cycle Engine for polygeneration with MED Desalination, A preliminary approach, Energy Conversion and Management (2012) 53: 108-117.

[9] Al-Mutaz I. S., Wazeer I., Current Status and Future Directions of MED-TVC Desalination Technology, Desalin, Water Treatment (2014) 55: 1-9.

[10] Kashi A., Investigation of Energy Efficiency and Produced Water in Desalination Distillation Systems, International Water Technology Journal (2015) 5: 1-19.

[11] Ettouney H.M., El-Dessouky H. Fundamentals of Salt Water Desalination, Kuwait University (2002).

[12] Sharqawy M.H., Lienhard V J.H., Zubair S.M., On Exergy Calculations of Seawater with Applications in Desalination Systems, International Journal of Thermal Sciences (2011) 50: 187-196.

[13] Ashour M.M., Steady State Analysis of the Tripoli West LT-HT-MED Plant, Desalination (2002) 152: 191-194 .

[14] Al-Mutaz I.S., Wazeer I., Development of a Steady-State Mathematical Model for MEE-TVC Desalination Plants, Desalination (2014) 351: 9-18.

[15] MAPNA Group, Qeshm Water and Power Cogeneration Plant Data, Iran (2011).

Appendix A

The thermodynamic property of seawater can be found in the following section.

Specific volume

$$v_{sw} = \frac{1}{\rho_{sw}} \qquad (A.1)$$

$$\rho_{sw} = \rho_w + w_s \left(a_1 + a_2 T + a_3 T^2 + a_4 T^3 + a_5 w_s T^2 \right) \qquad (A.2)$$

$$\rho_w = 9.999 \times 10^2 + 2.034 \times 10^{-2} T - 6.162 \times 10^{-3} T^2 +$$
$$2.261 \times 10^{-5} T^3 - 4.657 \times 10^{-8} T^4$$
$$a_1 = 8.020 \times 10^2, \ a_2 = -2.001, a_3 = 1.677 \times 10^{-2},$$
$$a_4 = -3.060 \times 10^{-5}, a_5 = -1.613 \times 10^{-5} \qquad (A.3)$$

where v_{sw}, ρ_w, w_s, and T are seawater-specific volume, seawater and pure water density, salt salinity, and temperature, respectively.

Specific enthalpy

The specific enthalpy can be calculated as follows:

$$h_{sw} = h_w - w_s (b_1 + b_2 w_s + b_3 w_s^2 + b_4 w_s^3 + b_5 T^1 +$$
$$b_6 T^2 + b_7 T^3 + b_8 w_s T^1 + b_9 w_s^2 T^1 + b_{10} w_s T^2) \qquad (A.4)$$

$$h_w = 141.355 + 4202.070 \times T - 0.535 \times T^2 +$$
$$0.004 \times T^3 \qquad (A.5)$$

$$b_1 = -2.348 \times 10^4, b_2 = 3.152 \times 10^5, b_3 = 2.803 \times 10^6,$$
$$b_4 = -1.446 \times 10^7, b_5 = 7.826 \times 10^3, \ b_6 = -4.417 \times 10^1,$$
$$b_7 = 2.139 \times 10^{-1}, b_8 = -1.991 \times 10^4, b_9 = 2.778 \times 10^4, \qquad (A.6)$$
$$b_{10} = 9.728 \times 10^1$$
$$h_{sw} (T, P, w_s) = h_{sw} (T, P_0, w_s) + v (P - P_0)$$

Specific entropy

The following equation can be used for the calculation of seawater-specific entropy:

$$s_{sw} = s_w - w_s (c_1 + c_2 w_s + c_3 w_s^2 + c_4 w_s^3 + c_5 T^1 +$$
$$c_6 T^2 + c_7 T^3 + c_8 w_s T^1 + c_9 w_s^2 T^1 + c_{10} w_s T^2) \qquad (A.7)$$

$$s_w = 0.1543 + 15.383 \times T - 2.996 \times 10^{-2} T^2 +$$
$$8.193 \times 10^{-5} T^3 - 1.370 \times 10^{-7} T^4$$
$$c_1 = -4.231 \times 10^2, c_2 = 1.463 \times 10^4,$$
$$c_3 = -9.880 \times 10^4, \ c_4 = 3.095 \times 10^5,$$
$$c_5 = 2.562 \times 10^1, \ c_6 = -1.443 \times 10^{-1}, \qquad (A.8)$$
$$c_7 = 5.879 \times 10^{-4}, c_8 = -6.111 \times 10^1,$$
$$c_9 = 8.041 \times 10^1, c_{10} = 3.035 \times 10^{-1}$$

Chemical potential

The salt and water chemical potential in seawater can be calculated by differentiating the Gibbs energy with respect to its composition as follows:

$$\mu_w = \frac{\partial G_{sw}}{\partial m_w} = g_{sw} - w_s \frac{\partial g_{sw}}{\partial w_s} \qquad (A.9)$$

$$\mu_s = \frac{\partial G_{sw}}{\partial m_s} = g_{sw} + (1 - w_s) \frac{\partial g_{sw}}{\partial w_s} \qquad (A.10)$$

$$g_{sw} = h_{sw} - (T + 273.15) s_{sw} \qquad (A.11)$$

, where, μ *and* G are the chemical potential and the Gibbs energy, respectively.

$$\frac{\partial g_{sw}}{\partial w_s} = \frac{\partial h_{sw}}{\partial w_s} - (T + 273.15) \frac{\partial s_{sw}}{\partial w_s} \qquad (A.12)$$

$$-\frac{\partial h_{sw}}{\partial w_s} = b_1 + 2b_2 w_s + 3b_3 w_s^2 + 4b_4 w_s^3 + b_5 T +$$
$$b_6 T^2 + b_7 T^3 + 2b_8 w_s T + 3b_9 w_s^2 T + 2b_{10} w_s T^2 \qquad (A.13)$$

$$-\frac{\partial s_{sw}}{\partial w_s} = c_1 + 2c_2 w_s + 3c_3 w_s^2 + 4c_4 w_s^3 + c_5 T +$$
$$c_6 T^2 + c_7 T^3 + 2c_8 w_s T + 3c_9 w_s^2 T + 2c_{10} w_s T^2 \qquad (A.14)$$

Therefore, the flow exergy can be expressed as follows:

$$e_f = (h - h^*) - T_0 (s - s^*) + \sum_{i=1}^{n} (\mu_i^* - \mu_i^0) \qquad (A.15)$$

On the right-hand side of Equation 60, parts one and two are related to physical exergy, while the third part is related to the chemical exergy. In the above equation, the environmental temperature and pressure, and the initial state concentration (named restricted dead state) have been specified with the "*" sign. In environmental temperature, pressure, and concentration (named the dead state), the "0" sign has been used.